Fluorine-Containing Photoreactive Polyimides. 6. Synthesis and Properties of a Novel Photoreactive Polyimide Based on Photoinduced Acidolysis and the Kinetics for Its Acidolysis

Toshihiko Omote,* Ken'ichi Koseki, and Tsuguo Yamaoka

Department of Image Science and Technology, Faculty of Engineering, Chiba University, 1-33, Yayoi-cho, Chiba-shi 260, Japan

Received October 31, 1989

ABSTRACT: Polyimide (6FDA-AHHFP) prepared from the polycondensation of fluorinated acid dianhydride (6FDA) and diamine (AHHFP) is soluble in an aqueous base due to the presence of a hydroxyl group in the phenyl group of the diamine segment. Easy acidolysis of the protecting groups of the hydroxyl group was demonstrated with several model compounds of the polyimide that were protected by a number of acyl- and (alkyloxy)carbonyl groups. The *tert*-butoxycarbonyl group showed the highest acidolysis rate in these tests. A polyimide (6F-*t*-BOC) with a *tert*-butoxycarbonyl (*t*-BOC) group was thus prepared. On the basis of the results obtained from the model compound, it was expected that 6F-*t*-BOC would have a high sensitivity because the *t*-BOC group, as the protecting group, showed the highest acidolysis rate. Although 6F-*t*-BOC is insoluble in an aqueous base, it is easily converted to an alkaline-soluble polyimide by the acidolysis of this *t*-BOC group. This implies that polyimide 6F-*t*-BOC acts as a positive-working photoreactive material in the presence of a photoacid generator. Actually, 6F-*t*-BOC in the presence of (*p*-nitrobenzyl)-9,10-diethoxyanthracene-2-sulfonate (NBAS) as a photo acid generator showed excellent positive-working characteristics in an aqueous base developer because of the polarity change induced by removing the *t*-BOC group. The sensitivity and contrast after a postexposure bake at 120 °C for 10 min were 180 mJ/cm^2 (365 nm) and 3.4. Resolution higher than 1.0 μm was obtained in the 5-μm-thick film. The kinetics of thermolytically deprotecting the 6F-*t*-BOC film, when catalyzed by *p*-toluenesulfonic acid (*p*-Tos), was studied further in its solid state. The results clearly indicated that the reaction was first order, suggesting it was a typical A_{AL}-1 type reaction requiring no water. The activation energy for the acidolysis was 19.5 kcal/mol. It further became apparent that the diffusion radius of an acid in a 6F-*t*-BOC film containing *p*-Tos was ca. 14.2 Å when heated for 10 min at 80 °C. 6F-*t*-BOC has 2 mol of *t*-BOC groups per repeating unit. Examination of their thermolytic acidolysis showed that acidolysis of the first *t*-BOC group proceeded more slowly than that of the second one in each repeating unit. This was attributed to the fact that an acid could attack the second *t*-BOC group easier than the first one and was responsible for the steric inhibition of *tert*-butyl groups around the *t*-BOC that protected an acid.

Introduction

Photoreactive polyimides are attracting interest as a means of simplifying semiconductor fabrication. We have reported several types of fluorinated photoreactive polyimides[1,2] and their precursors.[3-5] The processing of these materials was improved by their high optical transparency and solubility in common organic solvents. Soluble polyimides are more advantageous than their precursors because they require no thermal curing for imidization, which induces excessive volume contraction. However, the design of fully imidized photoreactive polyimides having a higher sensitivity than that of their precursors has been limited by such factors as the rigidity and strong electron-acceptor property of the imide carbonyl. The rigidity of the polyimide prevents free radical migration and significantly hinders the rate of polymerization. The strong electron-accepting capability of the imide carbonyl may hinder the formation of exciplex between electron-donating and -accepting type initiators.

Recent attention given to systems involving a polarity change induced by a photochemically generated acid, an advanced photoresist design in the field of microlithography, has engendered the design of dual-tone resist materials.[6] The major feature of these systems is their high sensitivity due to a catalytic reaction caused by photogenerated acid.

The present paper discusses the preparation and properties of a novel positive-type, photoreactive polyimide having protecting groups that can be deprotected by acid. The kinetics for the thermolytic acidolysis of the protecting group is also discussed.

Experimental Section

Materials. All of the solvents used in this study are commercially available and were used after being dehydrated with molecular sieves. 6FDA (American Hoechst Co. 6FDA E grade) was refluxed in acetic anhydride for 2 h, filtered, and then dried at 150 °C for 3 h prior to use. AHHFP (Central Glass Co., Ltd.) was purified by recrystallization from diethylene glycol dimethyl ether (diglyme) and dried at 35 °C under reduced pressure for 12 h before use. Other materials were from commercial sources and were not further purified.

Film Formation and UV Exposure. 6F-*t*-BOC and 15 wt % photoacid generator against the polymer were dissolved in diglyme. The solution was spun on a silicon wafer and dried at 90 °C for 30 min to form a photosensitive film layer. The film thickness was measured by the multiple-interference method with a Nikon surface finish microscope. Films were exposed to either 365- or 436-nm wavelength light with a filtered super high-pressure mercury lamp. Imagewise exposure was carried out in the contact mode with a quartz mask.

Measurements. IR spectra were measured on an Hitachi infrared spectrometer (Model 260-10). UV spectra of the films were recorded on a Hitachi spectrometer (Model 200-20). NMR spectra were recorded in deuterioacetone or deuteriochloroform on a JEOL GSX-400 (^{13}C) and a GSX-500 for (^{1}H) spectrometers. Thermal behavior was monitored by a Rigaku Denki Co. CN8085E1 thermal analyzer at 10 °C/min for TGA and DSC under normal atmospheric conditions. Molecular weights of the polymers were determined by a TOSO HLC-802UR gel permeation chromatography (GPC) with a TSK-GEL H type column (styrene gel column) at 40 °C in THF using styrene as a standard. A Shimadzu GC-4CPTF gas chromatograph with a silicone GE SE-3C column (Wako Pure Chemical Industries, Ltd.) was used to identify the products after thermolysis of the 6F-*t*-BOC.

0024-9297/90/2223-4788$02.50/0

Synthesis of the Base-Soluble Polyimide. The soluble polyimide (6FDA-AHHFP) precursor was prepared by the polycondensation of 10 g of 5,5′-[2,2,2-trifluoro-1-(trifluoromethyl)-ethylidene]bis-1,3-isobenzofurandione (6FDA) and 8.24 g of 2,2-bis(3-amino-4-hydroxyphenyl)hexafluoropropane (AHHFP) in 73 g of *N*-methyl-2-pyrrolidone (NMP) at room temperature for 12 h. *m*-Xylene (24 g) was added to the poly(amic acid) solution and heated at 150 °C for 1.5 h for thermal cyclization. During this step, the water generated by the ring-closure reaction was separated as the *m*-xylene azeotrope. After the reaction was complete, 6FDA-AHHFP was precipitated from the NMP solution with water and dried overnight at 40 °C under reduced pressure. IR (NaCl) OH at 3400 cm^{-1}, imide >C=O at 1780 cm^{-1}, imide C–N at 1380 cm^{-1}; ^1H NMR (acetone-d_6) δ 7.17 (d, 2 H, 5,5′-H of AHHFP), 7.38 (d, 2 H, 6,6′-H of AHHFP), 7.57 (s, 2 H, 2,2′-H of AHHFP), 7.89 (s, 2 H, 6,6′-H of 6FDA), 8.04 (d, 2 H, 4,4′-H of 6FDA), 8.11 (d, 2 H, 3,3′-H of 6FDA), 9.36 (s, 2 H, OH); ^{19}F NMR δ –63.91 (s, 6 F, F, of 6FDA), –64.76 (s, 6 F, F of AHHFP). Anal. Calcd for $C_{34}H_{14}O_6N_2F_{12}$: C, 52.7; H, 1.82; N, 3.61. Found: C, 52.58; H, 1.76; N, 3.77.

Synthesis of the Protected Polyimide. 6FDA-AHHFP (5 g) was dissolved in 90 g of tetrahydrofuran, and then 2.17 g of potassium *tert*-butoxide was added. The solution was mechanically stirred for 15 min at 0 °C, and 4.23 g of di-*tert*-butyl dicarbonate was added dropwise to the solution. The resulting gelatinous mixture was stirred for 6 h at room temperature and then poured into cold methyl alcohol (–15 °C) to precipitate 6FDA-AHHFP protected with the *tert*-butoxycarbonyl group (6F-*t*-BOC). The weight-average and number-average molecular weights of 6F-*t*-BOC were 390 000 and 134 000, respectively. IR (NaCl) CH_3 at 2980 cm^{-1}, imide >C=O at 1780 cm^{-1}, carbonate >C=O at 1770 cm^{-1}, imide C–N at 1380 cm^{-1}; ^1H NMR (acetone-d_6) δ 1.37 (s, 18 H, CH_3), 7.63 (d, 2 H, 6,6′-H of AHHFP), 7.65 (d, 2 H, 5,5′-H of AHHFP), 7.83 (s, 2 H, 2,2′-H of AHHFP), 7.92 (s, 2 H, 6,6′-H of 6FDA), 8.08 (d, 2 H, 4,4′-H of 6FDA), 8.16 (d, 2 H, 3,3′-H of 6FDA); ^{19}F NMR δ –64.0 (s, 6 F, F of 6FDA), –64.46 (s, 6 F, F of AHHFP). Anal. Calcd for $C_{44}H_{30}H_{10}N_2F_{12}$: C, 54.22; H, 3.10; N, 1.43. Found: C, 54.41; H, 3.02; N, 1.55.

Synthesis of *p*-Nitrobenzyl 9,10-Diethoxyanthracene-2-sulfonate.[7] Sodium anthraquinone-2-sulfonate (0.05 mol), 5 g of zinc powder, and 10 mL of ethyl alcohol were dissolved in 20 mL of a 20 wt % aqueous solution of sodium hydroxide at 80 °C. Diethyl sulfonate (30 mL) was then added to this solution dropwise. The solution was cooled to 5 °C in an ice bath, and the precipitate was separated by filtration and washed with 10 wt % aqueous sodium hydrogen sulfite (mixture of $NaHSO_3$ and $Na_2S_2O_5$) to remove the unreacted sodium anthraquinone-2-sulfonate. This precipitate was dissolved in boiled water, the insoluble zinc powder and zinc hydroxide were removed by filtration, and finally sodium 9,10-diethoxyanthracene-2-sulfonate was recrystallized twice from water. Sodium 9,10-diethoxyanthracene-2-sulfonate (10 g) and 10 g of PCl_5 were dispersed in 100 g of methylene chloride and stirred at 40 °C for 1 h. The methylene chloride solution was filtered, washed with water, dried, and evaporated to obtain 9,10-diethoxyanthracene-2-sulfonyl chloride. This compound was then recrystallized three times in benzene. The chloride, *p*-nitrobenzyl alcohol, and triethylamine at a ratio of 1.00 mol:1.10 mol:1.50 mol were dissolved in tetrahydrofuran and stirred for 24 h at room temperature. Under reduced pressure, the solution was washed with water, dried, and then evaporated to remove tetrahydrofuran. (*p*-Nitrobenzyl)-9,10-diethoxyanthracene-2-sulfonate (NBAS) was obtained by column chromatography with a Wako gel C-200 column (Wako Pure Chemical Industries, Ltd.) using chloroform as the eluent. MP 110–112 °C; IR (KBr) SO_3 at 1190 and 1375 cm^{-1}, NO_2 at 1343 cm^{-1}; ^1H NMR ($CDCl_3$) δ 1.53 and 1.54 (t, 6 H, CH_3), 4.14 and 4.19 (q, 4 H, CH_2 of ethoxy), 5.12 (s, 2 H, CH_2 of benzyl), 7.35 (d, 2 H, meta H of nitrobenzyl), 7.48–7.51 (m, 2 H, 6,7-H of anthracene), 7.62 (q, 1 H, 3-H of anthracene), 8.20 (m, 2 H, ortho H of nitrobenzyl), 8.22 (q, 2 H, 5,8-H of anthracene), 8.29 (q, 1 H, 4-H of anthracene), 8.84 (q, 1 H, 1-H of anthracene). Anal. Calcd for $C_{25}H_{23}O_7NS$: C, 62.36; H, 4.81; N, 2.91. Found: C, 62.40; H, 4.80; N, 2.94.

Synthesis of the Model Compounds. Acylated Series. Phthalic anhydride (1.62 g) was dissolved in 15 g of NMP. AHHFP (2 g) was then gradually added to this solution, and the reaction mixture was stirred for 20 h at room temperature. After the reaction, 0.04 mol of acyclic anhydride and 1.3 g of pyridine were added to the amic acid solution. The solution was then stirred and heated at 110 °C for 2 h. The resulting solution was poured into ice-cooled methyl alcohol. Filtration rendered a white powder compound (**1**: 3.3 g, 89%; **2**: 3.43 g, 83%; **3**: 3.72, 86%). Analytical data of the synthesized compounds are as follows:

1: mp (DSC) 280 °C; IR (KBr) ν(C=O) at 3100 cm^{-1}, imide ν(C=O) at 1780 cm^{-1}, acyl ν(C=O) at 1720 cm^{-1}; ^1H NMR ($CDCl_3$) δ 7.94 (q, 4 H, 1,1′,4,4′-H), 7.80 (q, 4 H, 2,2′,3,3′-H), 7.60 (d, 2 H, 6,6′-H), 7.50 (s, 2 H, 5,5′-H), 7.45 (d, 2 H, 7,7′-H), 2.17 (s, 6 H, CH_3). Anal. Calcd for $C_{33}H_{17}O_5N_2F_6$: C, 62.37; H, 2.70; N, 4.40. Found: C, 62.39; H, 2.68; N, 4.38.

2: mp (DSC) 194 °C; IR (KBr) ν(CH_3) at 3000 cm^{-1}, ν(CH) at 2950 cm^{-1}, imide ν(C=O) at 1780 cm^{-1}, acyl ν(C=O) at 1730 cm^{-1}; ^1H NMR ($CDCl_3$) δ 7.94 (q, 4 H, 1,1′,4,4′-H), 7.79 (q, 4 H, 2,2′,3,3′-H), 7.60 (d, 2 H, 7,7′-H), 7.50 (s, 2 H, 5,5′-H), 7.43 (d, 2 H, 7,7′-H), 2.65 (m, 2 H, H of CH), 1.12 (d, 12 H, H of CH_3). Anal. Calcd for $C_{35}H_{21}O_5N_2F_6$: C, 63.35; H, 3.19; N, 4.22. Found: C, 63.40; H, 3.12; N, 4.23.

3: mp (DSC) 275 °C; IR (KBr) ν(CH_3) at 2980 cm^{-1}, imide ν(C=O) at 1790 cm^{-1}, acyl ν(C=O) at 1720 cm^{-1}; ^1H NMR ($CDCl_3$) δ 7.93 (q, 4 H, 1,1′,4,4′-H), 7.79 (q, 4 H, 2,2′,3,3′-H), 7.59 (d, 2 H, 6,6′-H), 7.50 (s, 2 H, 5,5′-H), 7.41 (d, 2 H, 7,7′-H), 1.15 (s, 18 H, CH_3). Anal. Calcd for $C_{36}H_{23}O_5N_2F_6$: C, 63.81; H, 3.42; N, 4.13. Found: C, 63.88; H, 3.40; N, 4.09.

(Alkyloxy)carbonyl Series Except 7. Phthalic anhydride (8.13 g) was gradually added to a solution of 10.05 g of AHHFP dissolved in 43 g of NMP in a dry nitrogen atmosphere. The reaction mixture was stirred for 12 h at room temperature. *m*-Xylene (30 g) was added to the amic acid solution, which was heated at 150 °C for 1.5 h in a dry nitrogen atmosphere for thermal cyclization. During this step, the water generated by the ring-closure reaction was separated as the *m*-xylene azeotrope. After the reaction was complete, the solution was poured into water, and the precipitate (6F-2OH) was filtered off and dried under reduced pressure. Triethylamine (0.97 g) was added dropwise to a solution of 2 g of 6F-2OH, and 9.6 mmol of alkyl chloroformate was dissolved in diglyme. The reaction mixture was stirred for 12 h at room temperature. The ammonium salt precipitate was then filtered off, and the filtrate was poured into methyl alcohol. Filtration gave a white powder product (**4**: 1.69 g, 71%; **5**: 1.74 g, 68%; **6**: 1.72 g, 65%).

4: mp (DSC) 257 °C; IR (KBr) ν(CH_3) at 2970 cm^{-1}, imide ν(C=O) at 1790 cm^{-1}, carbonate ν(C=O) at 1740 cm^{-1}; ^1H NMR (acetone-d_6) δ 7.95 (m, 8 H, 1,1′,2,2′,3,3′,4,4′-H), 7.80 (s, 2 H, 5,5′-H), 7.73 (d, 2 H, 6,6′-H), 7.65 (d, 2 H, 7,7′-H), 3.81 (s, 6 H, CH_3). Anal. Calcd for $C_{33}H_{17}O_6N_2F_6$: C, 60.84; H, 2.63; N, 4.30. Found: C, 60.90; H, 2.60; N, 4.23.

5: mp (DSC) 165 °C; IR (KBr) ν(CH_3) at 3000 cm^{-1}, ν(CH) at 2950 cm^{-1}, imide ν(C=O) at 1780 cm^{-1}, carbonate ν(C=O) at 1740 cm^{-1}; ^1H NMR ($CDCl_3$) δ 7.93 (q, 4 H, 1,1′,4,4′-H), 7.79 (q, 4 H, 2,2′,3,3′-H), 7.60 (d, 2 H, 6,6′-H), 7.51 (s, d, 4 H, 5,5′,7,7′-H), 4.95 (m, 2 H, CH), 1.29 (d, 12 H, CH_3). Anal. Calcd for $C_{35}H_{21}O_6N_2F_6$: C, 61.86; H, 3.11; N, 4.12. Found: C, 61.88; H, 3.05; N, 4.17.

6: mp 179 °C; IR (KBr) ν(CH_3) at 2980 cm^{-1}, imide ν(C=O) at 1780 cm^{-1}, carbonate ν(C=O) at 1740 cm^{-1}; ^1H NMR ($CDCl_3$) δ 7.92 (q, 4 H, 1,1′,4,4′-H), 7.79 (q, 4 H, 2,2′,3,3′-H), 7.61 (d, 2 H, 6,6′-H), 7.52 (s, d, 4 H, 5,5′,7,7′-H), 4.01 (d, 4 H, CH_2), 1.98 (m, 2 H, CH), 0.91 (d, 12 H, CH_3). Anal. Calcd for $C_{36}H_{23}O_6N_2F_6$: C, 62.34; H, 3.34; N, 4.40. Found: C, 62.40; H, 3.33; N, 4.10.

Model Compound 7. A solution of 2 g of 6F-2OH in dry THF was treated with 1.07 g of potassium *tert*-butoxide. After a few minutes of stirring at room temperature, 2.09 g of di-*tert*-butyl dicarbonate was added, and the mixture was stirred for 6 h at room temperature. The resulting mixture was poured into ice-cooled methyl alcohol. Filtration gave the white powder product **7** (1.35 g, 51%).

7: mp 152 °C; IR (KBr) ν(CH_3) at 3000 cm^{-1}, imide ν(C=O) at 1790 cm^{-1}, carbonate ν(C=O) at 1770 cm^{-1}; ^1H NMR ($CDCl_3$) δ 7.93 (q, 4 H, 1,1′,4,4′-H), 7.78 (q, 4 H, 2,2′,3,3′-H), 7.58 (d, 2 H, 6,6′-H), 7.50 (s, 2 H, 5,5′-H), 7.47 (d, 2 H, 7,7′-H), 1.45 (s, 18 H, CH_3). Anal. Calcd for $C_{36}H_{23}O_6N_2F_6$: C, 62.34; H, 3.34; N, 4.40. Found: C, 62.38; H, 3.36; N, 4.11.

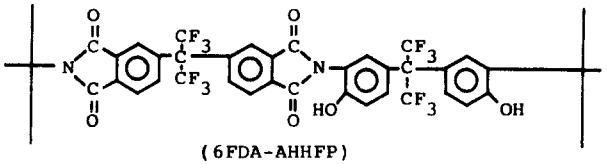

(6FDA-AHHFP)

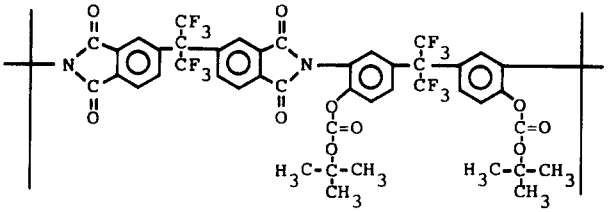

(6F-t-BOC)

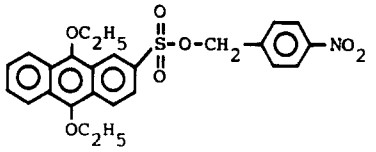

(NBAS)

Figure 1. Chemical structures of the synthesized polyimides and photo acid generator used in this study.

Results and Discussion

Ease of Removal of Protecting Group. The base polyimide 6FDA-AHHFP shows high solubility not only in common polar organic solvents but also in aqueous bases and mixed solutions of alcohol and an aqueous base, depending on the molecular weight. However, the solubility of 6FDA-AHHFP in an aqueous base or alcohol is diminished by protecting the hydroxyl group. The solubility difference resulting from this polarity change suggests that the protected polyimide may allow the design of highly sensitive positive-working resist materials incorporating a chemical amplification process. To study the acidolytic capability of the 6FDA-AHHFP protecting group, a series of model compounds corresponding to this unit of the polyimide were prepared and protected with various protecting groups.

Concentrated sulfuric acid (1.6×10^{-3} mol) and 4.7×10^{-3} mol of water were added to a solution of 0.1 g of each model compound dissolved in 3 mL of *N,N*-dimethylacetamide. The solution was heated for 30 min at a specific temperature and then poured into water to precipitate a mixture of the protected and deprotected model compounds. The ratio of the protected and deprotected model compound in the precipitate was determined by the OH peak and the peak of the proton of each protecting group in the ^1H NMR spectrum[8a] (Figure 2). From this result, it was found that the acidolytic facility of protecting groups at a heating temperature of 150 °C was in the order $COCH_3 > COCH(CH_3)_2 > COC(CH_3)_3$ for the acylated series and $OCOC(CH_3)_3 > OCOCH_3 > OCOCH_2CH(CH_3)_2 > OCOCH(CH_3)_2$ for the alkyloxycarbonylated series. In the case of the acylated series, it seemed that the acidolytic capability was governed by the steric factor of the protecting groups. Consequently, the mechanism of this acidolysis can be explained by an A_{AC}-2 reaction. With respect to the alkyloxycarbonylated series, however, a well-defined relationship between the ease of acidolysis and the structure of the compound could not be found. This result may be due to different mechanisms operating at the same time.

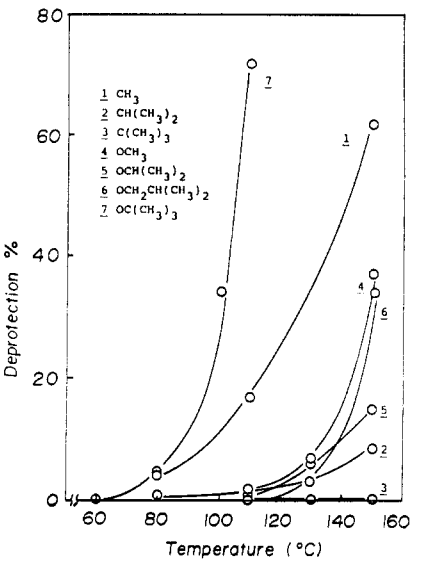

Figure 2. Thermolytic acidolysis for various protecting groups of the model compounds.

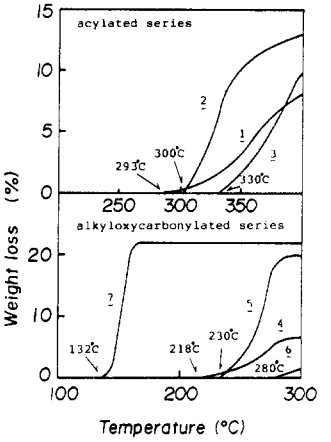

Figure 3. Thermal deprotecting temperatures for various model compounds.

The thermal decomposition starting temperatures of model compounds, which were measured by TGA curves, are shown in Figure 3. These results clearly indicate that the ease of deprotection of the model compounds in Figure 2 is due to acidolysis and not to thermolysis.

Sensitivities. On the basis of the results obtained from the model compound reaction, polyimide 6F-*t*-BOC, derived by protecting a hydroxyl group of 6FDA-AHHFP with a *t*-BOC group, was synthesized by the method described in the Experimental Section. The lithographic performance of 6F-*t*-BOC was studied by using NBAS as a photo acid generator. The electronic absorption band of NBAS extending to 436 nm (*g* line) is photobleached due to the addition of singlet oxygen to the 9,10-positions of anthracene. NBAS is photochemically decomposed to give 9,10-diethoxyanthracene-2-sulfonic acid, which is strongly acidic and catalyzes the thermolysis of 6F-*t*-BOC's *t*-BOC group (Scheme I).[7]

6F-*t*-BOC films (1 μm thick) containing 15 wt % NBAS became soluble in an aqueous base by exposure to UV light and successive postexposure bakes (PEB) in the temperature range 100–120 °C. The sensitivity (D^0) and contrast (γ^0) of 6F-*t*-BOC were evaluated by the characteristic curves. D^0 and γ^0 were 270 mJ/cm^2 and 4.2 with 365-nm light and 650 mJ/cm^2 and 2.7 with 436-nm light with PEB at 110 °C for 10 min. Furthermore, with 365-nm light with PEB at 120 °C for 10 min, they were

Scheme I
Photochemical Reaction of NBAS

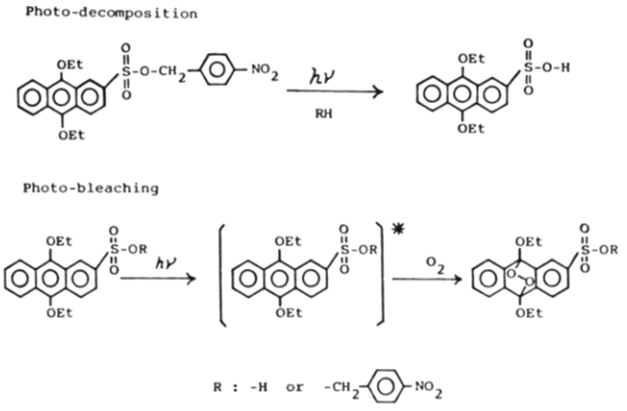

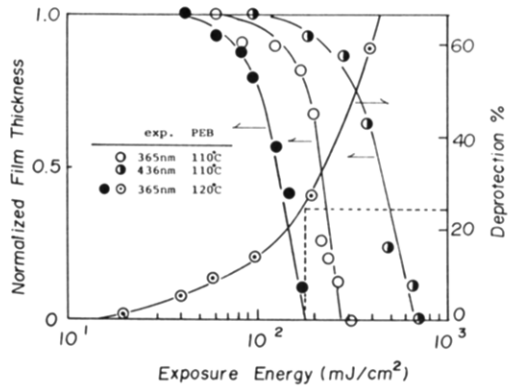

Figure 4. Sensitivity plot for 6F-*t*-BOC containing NBAS and deprotecting ratio of the *t*-BOC group on exposure.

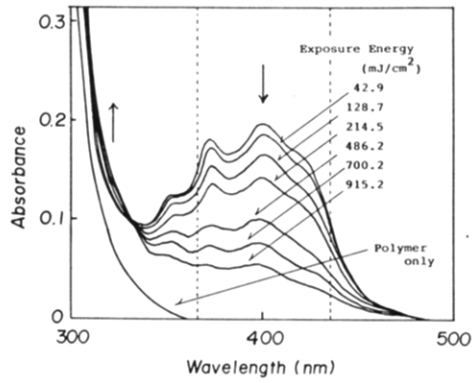

Figure 5. Electronic spectral change of the 6F-*t*-BOC film with NBAS on exposure.

enhanced to 180 mJ/cm² and 3.4 (Figure 4). The amount of 6F-*t*-BOC photodeprotection in a film was determined by the OH proton peaks at δ 9.37 and 9.43 and the $(CH_3)_3$ peak at δ 1.37 in the ^1H NMR spectra.[8b] From this quantitative analysis, it was also found that 24 mol % of hydroxyl groups were deprotected with exposure and PEB conditions at D^0 (also Figure 4).

Patterning Characteristics. Figure 5 shows the electronic spectrum of 6F-*t*-BOC film containing 15 wt % NBAS and the resulting change at exposure to 365-nm wavelength. 6F-*t*-BOC has no absorption wavelength longer than 360 nm. The absorption peaks at 400 nm, which result from NBAS, rapidly bleach on exposure even in the solid state. This spectral behavior on exposure suggests that 6F-*t*-BOC may produce excellent patterns from even a thick film by using NBAS as a sensitizer. Figure 6 shows a scanning electron micrograph (SEM) of the positive pattern printed in a 5μm-thick of 6F-*t*-BOC

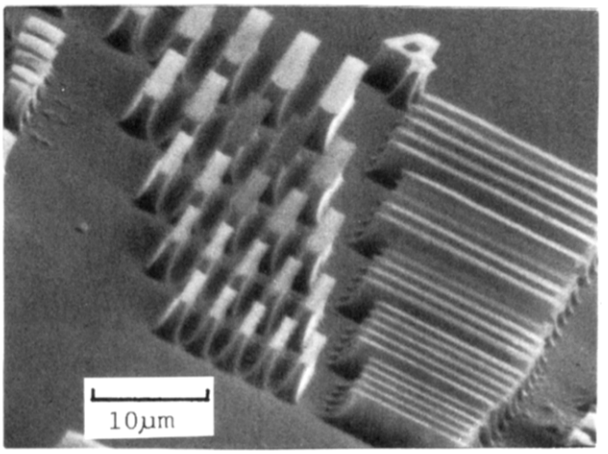

Figure 6. Scanning electron micrograph of the pattern contact printed in 6F-*t*-BOC with NBAS.

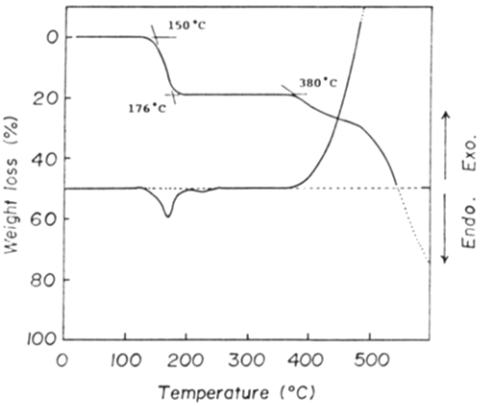

Figure 7. Thermal behavior of 6F-*t*-BOC on TGA and DSC curves.

film with 15 wt % NBAS. A high-resolution pattern, finer than 1 μm and with a good profile, is observed in the SEM photograph.

Deprotecting Reaction of the *t*-BOC Group from 6F-*t*-BOC. The thermal behavior of 6F-*t*-BOC, which showed excellent patterning characteristics, was observed by TGA and DSC curves (Figure 7). Two downward slopes, one representing a sharp endothermic mass loss between 150 and 176 °C and the other an exothermic mass loss starting at around 380 °C, are observed in the curves. The 20% mass loss of the first drop very closely correponds to the *t*-BOC's mass percent of the total 6F-*t*-BOC mass.

The IR spectra of the polymer films after heating at 50 °C (A) and at 200 °C (B) for 15 min are indicated in Figure 8. The ^{13}C NMR spectra of the polymers after heating at 50 °C and at 200 °C for 15 min are shown in Figure 9. IR spectrum A has a sharp carbonyl band at 1770 cm^{-1} due to carbonate and no hydroxyl absorption at 3400 cm^{-1}. IR spectrum (B) has a decreased carbonyl band at 1770 cm^{-1} due to carbonate and a broad hydroxyl band at 3400 cm^{-1}. The ^{13}C NMR spectra A and B are assigned to 6F-*t*-BOC and 6FDA-AHHFP, respectively (Figure 9). The first drop of the TGA curves in Figure 7 must therefore represent the deprotecting reaction of the *t*-BOC group from the 6F-*t*-BOC. The reaction involving the removal of the *t*-BOC group from 6F-*t*-BOC was investigated by gas chromatography. From this analysis, it was concluded that the *t*-BOC group is converted to carbon dioxide and 2-methylpropene (Scheme II), and the reaction in acid-catalyzed thermolysis is exactly the same as that in thermolysis.

Removal Behavior and Mechanism of the *t*-BOC Group. It is interesting to study how the protecting groups

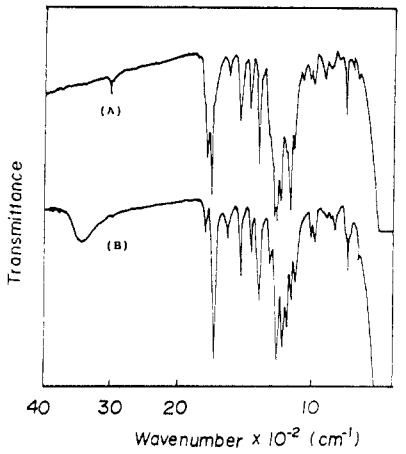

Figure 8. IR spectra of 6F-*t*-BOC films after heating at 50 °C (A) and at 200 °C (B) for 15 min.

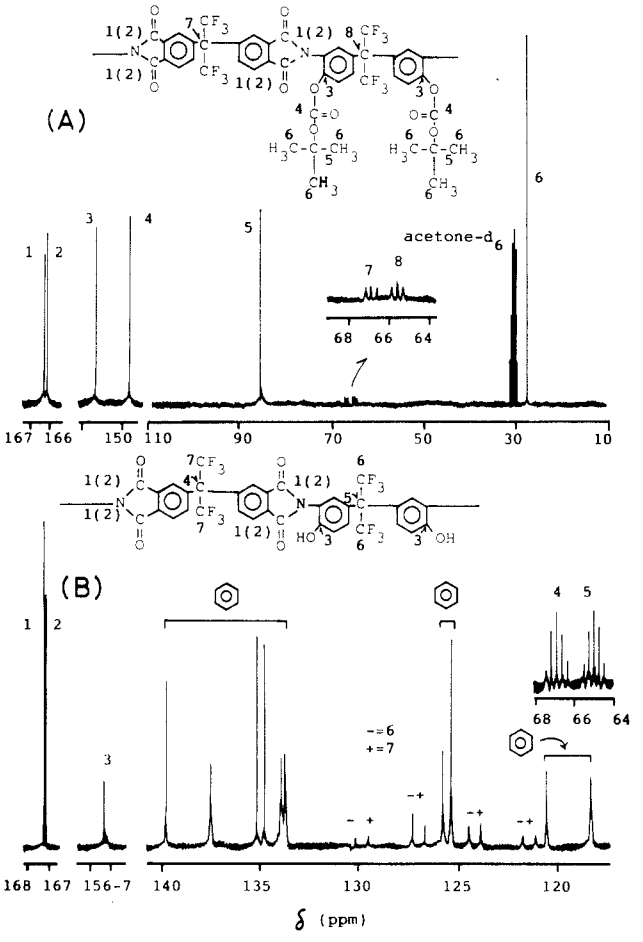

Figure 9. ^{13}C NMR spectra (in acetone-d_6) of 6F-*t*-BOC after heating at 50 °C (A) and at 200 °C (B) for 15 min.

Scheme II
Deprotecting Reaction Scheme of 6F-*t*-BOC

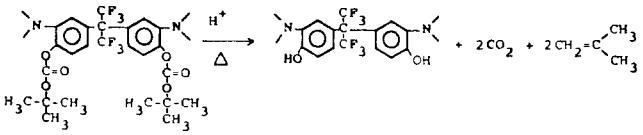

in 6F-*t*-BOC are released by acidolysis in the solid state. Polymer films containing 0.12 mol/L *p*-toluenesulfonic acid monohydrate (*p*-Tos) were coated on glass substrates and dried at 30 °C for 24 h under reduced pressure. These dried films were dissolved in acetone after heating at several temperatures, and then the polymer solution were precipitated with water. The deprotection ratio was

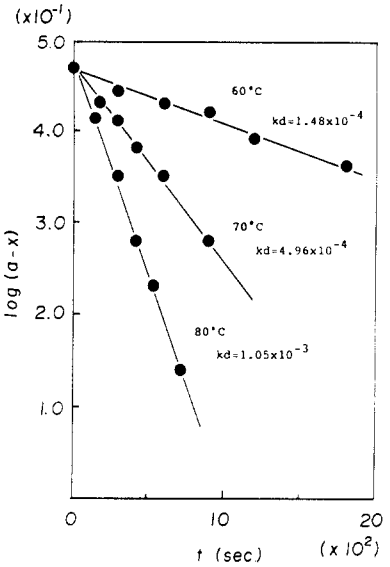

Figure 10. First-order kinetic plots of log $(a - x)$ versus reaction time for thermolytic acidolysis of the 6F-*t*-BOC film with *p*-Tos.

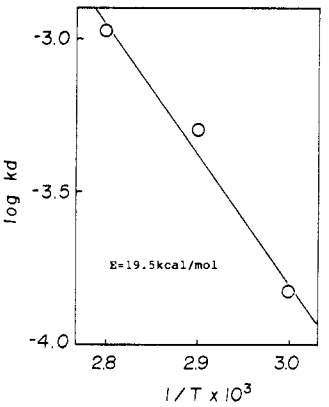

Figure 11. Arrhenius plot for thermolytic acidolysis of the 6F-*t*-BOC film with *p*-Tos.

determined by the weight loss at the first drop in the TGA curves. log $(a - x)$ is plotted against the heating time in Figure 10. Here, a represents the initial concentration of *t*-BOC groups, while x is the concentration of removed groups in the film. The concentrations of the *t*-BOC group and acid in the film were calculated by estimating that the density of 6F-*t*-BOC film is 1.4. The straight line indicates that the *t*-BOC group in 6F-*t*-BOC readily undergoes an acid-catalyzed deprotecting reaction that does not require a stoichiometric amount of water. The activation energy for the deprotecting reaction in the solid state was estimated at 19.5 kcal/mol from an Arrhenius plot (Figure 11).

Deprotected *t*-BOC concentration is plotted as a function of the reaction time at 80 °C for several concentrations of *p*-Tos in the film (Figure 12). Within the time range shown in the figure, higher acid concentration in the film induces a faster deprotection of *t*-BOC from 6F-*t*-BOC. However, at lower acid concentration, more of the *t*-BOC group was actually deprotected per mole of acid at the reaction time of 600 s. For example, 1 mol of acid in 0.05 mol/L *p*-Tos deprotected as much as 21 mol of *t*-BOC groups, while 1 mol of acid in 0.55 mol/L *p*-Tos deprotected 5.5 mol of *t*-BOC groups by heating for 10 min at 80 °C. The diffusion volume of an acid by heating does not depend on the acid concentration in the film. Therefore, the above result must be due to the diffusion volume of each acid overlapping in the case of higher acid concentrations. Before thermolytic acidolysis of the *t*-BOC

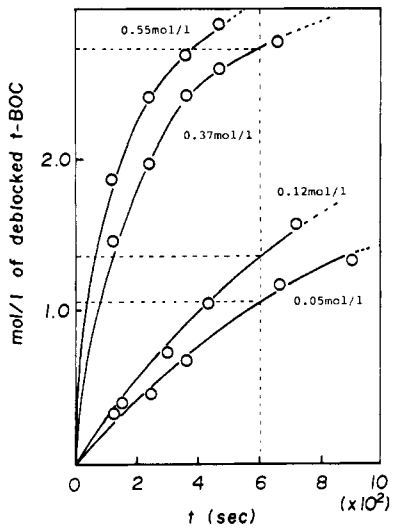

Figure 12. Plots of the protected *t*-BOC group concentration versus thermolytic acidolysis reaction time of the 6F-*t*-BOC film with several concentrations of *p*-Tos.

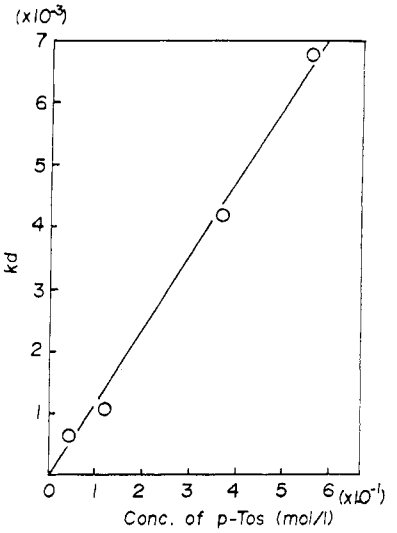

Figure 13. Relationship between k_d and *p*-Tos concentration for thermolytic acidolysis of the 6F-*t*-BOC film.

group, 1.73×10^{24} molecules of the *t*-BOC groups exist in a liter of the homogeneous 6F-*t*-BOC film, with *p*-Tos having a density estimated at 1.4. Consequently, the possible diffusion volume of an acid made by heating for 10 min at 80 °C would be larger than the 1.21×10^4 Å^3 volume occupied by 21 molecules of the *t*-BOC groups. The diffusion radius of an acid would be longer than 14.2 Å, as its diffusion rate in the film is isotropic. With an acid concentration of 0.05 mol/L in film, the number of acids per liter is ca. 3.01×10^{22}. If the diffusion volume of an acid is 1.21×10^4 Å^3, the total diffusion volume of 0.05 mol of acid will be 3.64×10^{26} Å^3 $\ll 1.0 \times 10^{27}$ Å^3 = 1 L, and the diffusion volume for each acid will not overlap one another. The diffusion radius of an acid in 6F-*t*-BOC film with *p*-Tos is therefore determined to be ca. 14.2 Å through the chemical amplification process when heated for 10 min at 80 °C. This result provides interesting observations about the fundamental behavior of an acid in the solid state as well as the patterning characteristics of resist materials incorporating a chemical amplification process. With regard to the lithographic performance, excess acid diffusion during heating would result in the loss of resolution. However, its radius was only 14.2 Å in this study, showing one reason 6F-*t*-BOC with an acid-generator offers such an excellent pattern as shown in Figure 6.

The relationship between the rate constant of deprotection (k_d), which was calculated by the slope of the first-order plots, and the concentration of *p*-Tos in the film is shown in Figure 13. From this straight line, it is noted that the deprotection is a first-order reaction against the term of the acid concentration also, and the attack of protons on the *t*-BOC groups is the rate-determining step of this reaction.

Polymer Structural Influence on Removal of the *t*-BOC Group. The soluble polyimides were synthesized from several acid dianhydrides having different structures to investigate the effect of structure on the deprotecting reaction. The resulting polymer structures are shown in Table I. The first-order plots for the thermolytic deprotecting reaction of these polymers, catalyzed by *p*-Tos, display good straight lines as shown in Figure 14, and the order of k_d was 6F-*t*-BOC > BT-*t*-BOC > DS-*t*-BOC. Since k_d for 6F-*t*-BOC was entirely uninfluenced by differences in molecular weight between 10 000 and 390 000, consideration of the molecular weight differences among these

Table I
Chemical Structures and Molecular Weights of Synthesized Polyimides with the *t*-BOC Group and Different Acid Dianhydride Segments

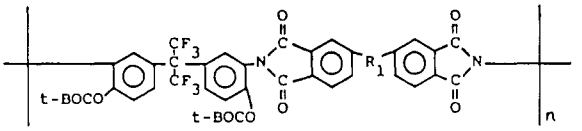

R	$\bar{M}_w$	$\bar{M}_n$	abbrev
$-C(CF_3)_2-$	14 400	8 300	6F-*t*-BOC
	392 300	133 900	
$-SO_2-$	81 800	53 800	DS-*t*-BOC
-CO-	22 300	11 800	BT-*t*-BOC

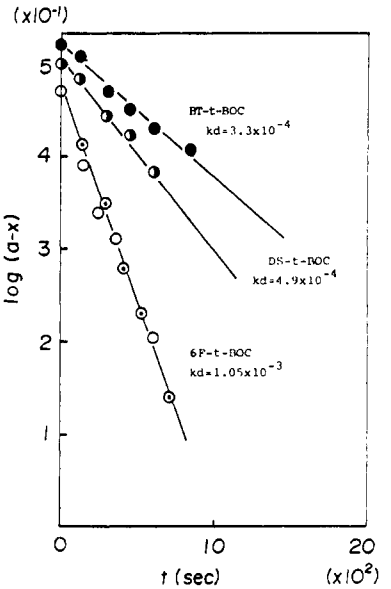

Figure 14. First-order kinetic plots of log $(a - x)$ versus reaction time for thermolytic acidolysis of polyimides having different acid dianhydride segments: (○) $\bar{M}_w$ = 14 400; (⊙) $\bar{M}_w$ = 392 300).

polymers is not relevant to the above result. In order to elucidate an electronic effect on this result, the pH value of each polymer having no protecting groups was measured in a solution of acetonitrile and water in a ratio of 4/1 (vol/vol). The concentration of the repeating unit for each polymer was 2×10^{-4} mol/L. A good relationship between the pH value and k_d was obtained (Figure 15). The acidity of the polymers depends on the potency of the electron-withdrawing effects of the substituents at the ortho position

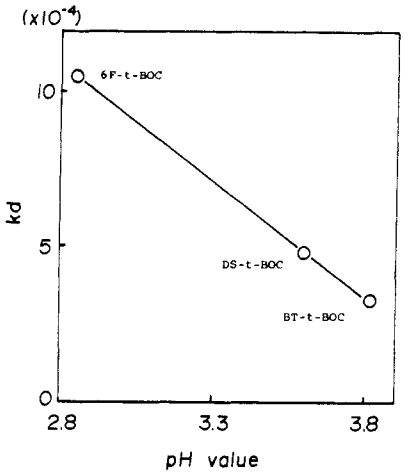

Figure 15. Relationship betwen k_d and pH values for three kinds of polyimides.

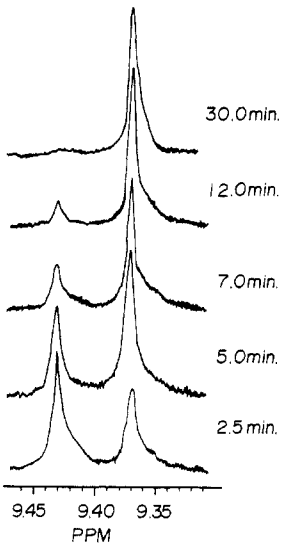

Figure 16. ^{1}H NMR spectral change of 6F-*t*-BOC according to heating time at 80 °C.

of the hydroxyl group. The stronger electron-withdrawing effect of the acid dianhydride segments therefore induces the faster deprotection rate of the *t*-BOC group. This also clearly indicates that the deprotection for the polyimide in the solid state is an A_{AL}-1 type thermolytic acid-catalyzed reaction.

Studies of the Deprotection of Two *t*-BOC Groups in a Repeating Unit. The ^{1}H NMR spectral change of 6F-*t*-BOC attributed to an acidolytic deprotecting reaction is shown in Figure 16. Two ^{1}H NMR absorption peaks for the hydroxyl protons are at δ 9.37 and 9.43 in the beginning of the deprotecting reaction; later they become one peak at δ 9.37, which is identical with that of 6FDA-AHHFP. Furthermore, the model compound that was end capped by phthalic anhydride also showed a similar ^{1}H NMR spectrum. Hence, the peak at δ 9.43 in the ^{1}H NMR spectrum indicates the hydroxyl group deprotecting only one of the *t*-BOC groups, while the δ 9.37 peak marks the deprotection of both *t*-BOC groups in a 6F-*t*-BOC repeating unit. From ^{1}H NMR spectra, it is possible to estimate the kinetic behavior of deprotection for each *t*-BOC group in a repeating unit. In this case, the two rate constants for the deprotecting reaction, k_1' and k_2', can be written as the following three kinetic differential equations:

$$\underset{A}{OR\text{–}OR} \xrightarrow{k_1'} \underset{B}{OR\text{–}OH} \xrightarrow{k_2} \underset{C}{OH\text{–}OH}$$

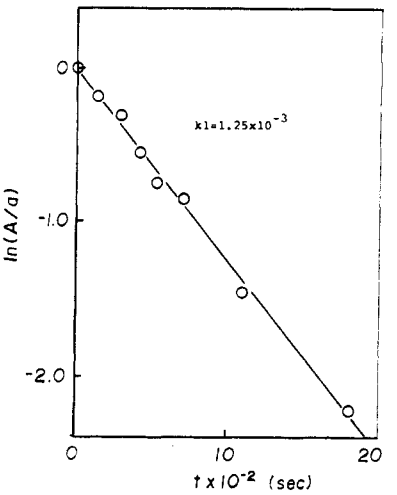

Figure 17. First-order kinetic plots of ln (A/a) versus reaction time for the deprotecting reaction of the first *t*-BOC in the 6F-*t*-BOC repeating unit.

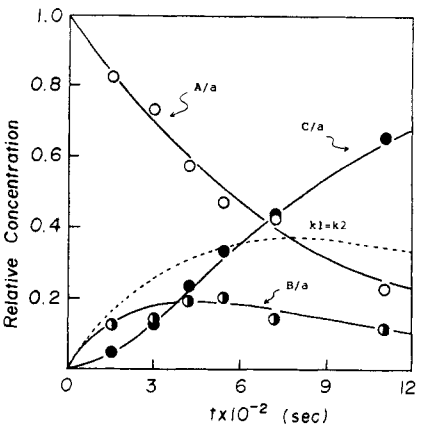

Figure 18. Composition of deprotected species as a function of heating time at 80 °C in the solid state: solid line, theoretical value; dashed line, if $k_1 = k_2$; circles, experimental data.

$$dA/dt = -k_1'A \quad (1)$$

$$dB/dt = k_1'A - k_2B \quad (2)$$

$$dC/dt = k_2B \quad (3)$$

where A, B, and C are the concentrations of OR–OR, OR–OH, and OH–OH, respectively, and their sums are equal. Equation 1 can be solved in terms of A assuming that the initial concentration of A is equal to a and $B = C = 0$ as shown in eq 4.

$$A = a\exp(-k_1't) \quad (4)$$

From eqs 2 and 4

$$B = k_1'a[\exp(-k_1't) - \exp(-k_2t)]/k_2 - k_1' \qquad (k_1' \neq k_2) \quad (5)$$

$$B = k_1'at\exp(-k_1't) \qquad (k_1' = k_2) \quad (6)$$

$$C = a - A - B \quad (7)$$

ln (A/a) was plotted against the heating time at 80 °C for 6F-*t*-BOC with 5 wt % *p*-Tos (Figure 17). From the slope of this straight line, the deprotection rate constant k_1' of the first *t*-BOC in a repeating unit was determined to be 1.25×10^{-3}. In Figure 18 the threoretical A/a and C/a values calculated by eqs 5 and 7 into which the k_1' value was substituted are illustrated by solid lines, and experimental data are indicated by circles. This result shows that the theoretical curves well reflected the experimental plots. Furthermore, the value of k_2 was determined as 3.8×10^{-3} by eq 5, which exactly simulates the experimental plot for B/a. As there are 2 mol of *t*-BOC groups in OR–OR which can be attacked by protons in the

initial stage, the real rate constant k_1 for deprotection of the first t-BOC is equal to $0.5k_1'$. It was consequently found that k_2 for the deprotection of the second t-BOC was 6 times larger than k_1. This fact clearly indicates that the rate-determining step of the deprotection is the attack of the acid against the first t-BOC group. Consequently, the straight line shown in Figure 10 is mainly due to the deprotection of the first t-BOC group and not significantly influenced by that of the second t-BOC group.

One possible explanation for $6k_1 = k_2$ is the local increase in acidity of the rigid polyimide film due to the hydroxyl group formed by the deprotection of the first t-BOC. To clarify this point, a similar experiment was also performed in a solution with the model compound containing the t-BOC group. The model compound (4.1×10^{-2} mol/L) and 1.6×10^{-1} mol/L of p-Tos was dissolved in dehydrated diglyme, and a compound was precipitated from the solution in water after heating at 80 °C. In the solution, it is not assumed that the hydroxyl group formed by the deprotection of the first t-BOC group selectively attacks only the second t-BOC group in the same molecule. The result was also $k_1 = 2.38 \times 10^{-4} < k_2 = 8.0 \times 10^{-4}$. Furthermore, the starting weight loss temperature of the partially deprotected model compound was exactly same as that of the untreated model compound in the TGA curves. The $6k_1 = k_2$ is thus not explained by a local increase in acidity. Since 6F-t-BOC consists of nonconjugated dianhydride (6FDA) and diamine (AHHFP), the neighboring t-BOC group is not electrically affected by the hydroxyl group through conjugation. Moreover, because the hydroxyl and t-BOC groups in a repeating unit are so distant, they cannot spatially interact. Judging from the above observations, we finally concluded that the difference between rate constants k_1 and k_2 was the result of the steric inhibition to acid of the *tert*-butyl groups around the t-BOC groups.

Conclusions

1. A novel photoreactive polyimide based on photoinduced acidolysis was prepared from polycondensation of the fluorinated acid dianhydride and diamine.

2. Ease of acid-catalyzed thermolysis of the protecting groups of the polyimide was investigated with its model compounds, and the t-BOC group was deprotected more easily than the other model compounds that were tested.

3. Polyimide 6F-t-BOC with NBAS offered an excellent pattern with a good profile and high sensitivity.

4. It was confirmed that the deprotecting reaction of 6F-t-BOC film catalyzed by acid was a typical A_{AL}-1 type reaction requiring no water.

5. The behavior of acids in the 6F-t-BOC film with p-Tos was studied, and it was found that the diffusion radius of an acid was 14.2 Å by heating for 10 min at 80 °C, which is a practical postexposure condition.

6. The facility of deprotection of the t-BOC group in the polyimide was very much dependent on the structure of the acid anhydride segments, and the acid dianhydrides having stronger electron-withdrawing groups showed faster acidolysis.

7. In a repeating polymer unit, the acidolysis of the first t-BOC group proceeded more slowly than that of the second group. This must cause the steric inhibition of the molecules around the t-BOC group that protect acids. The rate-determining step of the deprotecting reaction is thus the proton attack of the first t-BOC group.

References and Notes

(1) Omote, T.; Mochizuki, H.; Koseki, K.; Yamaoka, T. *Makromol. Chem., Rapid Commun.* **1989**, *10*, 521.
(2) Omote, T.; Mochizuki, H.; Koseki, K.; Yamaoka, T. *Polym. Commun.* **1990**, *31*, 133.
(3) Omote, T.; Yamaoka, T.; Koseki, K. *J. Appl. Polym. Sci.* **1989**, *38*, 389.
(4) Omote, T.; Koseki, K.; Yamaoka, T. *Polym. Eng. Sci.* **1989**, *29*, 14, 945.
(5) Omote, T.; Jin, G.; Koseki, K.; Yamaoka, T. *J. Appl. Polym. Sci.*, in press.
(6) See, for example: (a) Ito, H.; Willson, C. G. *Polym. Eng. Sci.* **1983**, *23*, 1012. (b) Ito, H.; Willson, C. G. In *Polymers in Electronics*; Davidson, T., Ed.; ACS Symposium Series 242; American Chemical Society: Washington, DC, 1984; p 11. (c) MacDonald, S. A.; Ito, H.; Willson, C. G. *Microelectron. Eng.* **1983**, 1, 269. (d) Ito, H.; Willson, C. G.; Frechet, J. M. J. *Proc. SPIE—Int. Soc. Opt. Eng.* **1987**, *771*, 24. (e) Osuch, C. E.; Brahim, K.; Hopf, F. R.; Mcfirland, M. J.; Mooring, A.; Wu, C. J. *Advances in Resist Technology and Processing* III: Willson, C. G., Ed.; *Proc. SPIE—Int. Soc. Opt. Eng.* **1986**, *631*, 68. Yamaoka, T.; Nishiki, M.; Koseki, K.; Koshiba, M. *Polym. Eng. Sci.* **1989**, *29*, 13, 856.
(7) Yamaoka, T.; Adachi, H.; Matsumoto, K.; Watanabe, Y.; Shirosaki, T. *J. Chem. Soc.*, in press.
(8) (a) In the ^{1}H NMR spectrum the signal intensity due to the hydroxyl group sometimes becomes weaker than the actual one because of the influence of water contained in the solvent and is not therefore reliable for quantitative analysis. However, a deuterio solvent containing only a little water was used in this study. The insignificance of the decrease in signal at δ 9.43–9.73 due to the hydroxy group was confirmed by comparing the integrations of δ 1.37 due to the *tert*-butyl group and δ 7.4–8.0 due to the aromatic rings. This comparison also shows that ^{1}H NMR is an appropriate technique. Furthermore, judging from the integrations of proton signals due to the aromatic rings and the *tert*-butyl groups, it is clear that the model compounds contained no free phenolic hydroxyl groups prior to these experiments. (b) The decrease in the signal was also negligible. The amount of t-BOC deprotection measured by the weight loss shown in TGA curves closely corresponded to that measured by ^{1}H NMR.